

# The Catalytic Acid in the Dephosphorylation of the Cdk2-pTpY/CycA Protein Complex by Cdc25B Phosphatase

Guilherme Menegon Arantes\*

Departamento de Bioquímica, Instituto de Química, Universidade de São Paulo, Av. Lineu Prestes 748, 05508-900 São Paulo, SP, Brasil

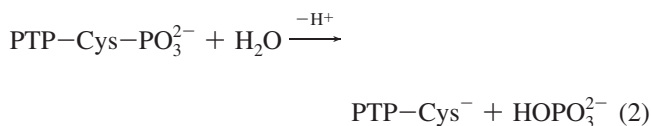
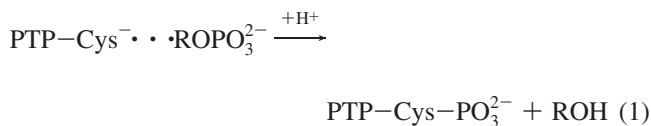
Received: August 5, 2008; Revised Manuscript Received: September 16, 2008

The development of anticancer therapeutics that target Cdc25 phosphatases is now an active area of research. A complete understanding of the Cdc25 catalytic mechanism would certainly allow a more rational inhibitor design. However, the identity of the catalytic acid used by Cdc25 has been debated and not established unambiguously. Results of molecular dynamics simulations with a calibrated hybrid potential for the first reaction step catalyzed by Cdc25B in complex with its natural substrate, the Cdk2-pTpY/CycA protein complex, are presented here. The calculated reaction free-energy profiles are in very good agreement with experimental measurements and are used to discern between different proposals for the general acid. In addition, the simulations give useful insight on interactions that can be explored for the design of inhibitors specific to Cdc25.

## 1. Introduction

Cdc25 phosphatases are crucial regulators of the eukaryotic cell cycle because they activate cyclin-dependent kinases (Cdk) responsible for cycle check points. Overexpression of Cdc25 phosphatases has been linked to diverse cancers.<sup>1</sup> Hence, these enzymes are now attractive targets for antineoplastic agents.<sup>2–4</sup> Because most drugs that target enzymes are competitive or irreversible inhibitors of active sites,<sup>5</sup> it is important that drug designers know the catalytic residues and understand the catalytic mechanism of the target enzyme.

Cdc25 phosphatases are protein tyrosine phosphatases (PTPs) of dual specificity.<sup>6</sup> They hydrolyze phosphotyrosine, phosphoserine, and phosphothreonine in two consecutive reactions. The first step is the nucleophilic attack from a PTP cysteine side chain toward the phosphate ester substrate, with a possible H<sup>+</sup> transfer from a general acid to the leaving group. A thiophosphorylated PTP intermediate is formed, and the substrate is dephosphorylated (eq 1). The PTP intermediate is hydrolyzed, and free enzyme is regenerated in the second step (eq 2).<sup>6–8</sup>



Almost all PTPs use as a general acid, an Asp residue located in a mobile loop (the WPD loop) at a distance from the active site.<sup>7</sup> Cdc25s are an exception to this observation. Structural studies have demonstrated that Cdc25s lack an Asp residue near the active site or in a flexible loop comparable to the WPD

loop in the other PTPs that could donate a H<sup>+</sup> to the leaving group.<sup>9,10</sup> Hence, the identity of the general acid on Cdc25s remains elusive. It has been suggested that the catalytic acid is a Glu residue (Glu474 on Cdc25B) located in the active site just after the catalytic cysteine (Cys473 on Cdc25B).<sup>9,11</sup> This Glu residue is conserved among all known Cdc25 isoforms.<sup>7</sup> Another proposal suggested that the substrate could bind as a phosphate monoanion and transfer the proton itself to the leaving group.<sup>12</sup> If well characterized, the difference in the catalytic acid between Cdc25 phosphatases and other PTPs could be explored in the design of inhibitors specific to Cdc25s.

In the following work, both proposals for the catalytic acid were tested via molecular dynamics simulations for the first reaction step (eq 1) of Cdc25B docked with its natural substrate, the protein complex Cdk2-pTpY/CycA, cyclin-dependent kinase 2 bis-phosphorylated and complexed with cyclin A.<sup>13</sup> This reaction corresponds to dephosphorylation of pThr14 on Cdk2 via a nucleophilic attack by Cys473 on Cdc25B. The next section gives details about the modeled structures and potentials used in the simulations. Calculated free-energy profiles shown in the Results and Discussion section are compared to the experimental rate constant and used to discern which proposal for the general acid is energetically feasible. In addition, interactions containing Glu474 are suggested as a new target for the design of inhibitors specific to Cdc25s.

## 2. Materials and Methods

Initial coordinates of a Cdc25B/Cdk2-pTpY/CycA model complex were kindly provided by J. Rudolph (Duke University). This model has been extensively validated via kinetic, mutagenic, X-ray crystallographic, and calorimetric studies.<sup>13</sup> The protein complex was solvated in a cubic water box of side 108.8 Å. The resulting system has a total of 129793 atoms, including 39263 water molecules, 4 Na<sup>+</sup> to neutralize the total charge, and 735 amino acids from the three proteins. This is a very large model structure as well as the first computer simulation of a phosphatase reaction with its natural substrate. The protonation state of each residue was the same as that adopted

\* E-mail: garantes@iq.usp.br.

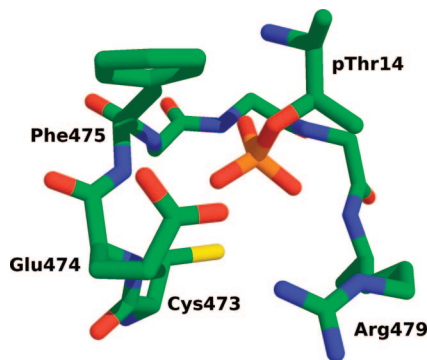


**Figure 1.** Snapshot of the simulated Michaelis complex. Only part of the P-loop heavy atoms are shown. Some side chains and parts of the backbone were erased to ease visualization.

by Rudolph et al.,<sup>13</sup> but the side chain of Glu474 was protonated, Ser473 was changed to Cys, and its side chain was ionized. This system was equilibrated for 1 ns of molecular dynamics simulation<sup>14</sup> at 300K and 1 atm using the Berendsen temperature and pressure couplings.<sup>15</sup> The protein complex and the solvent were represented with the OPLS-AA<sup>16</sup> and TIP-3P<sup>17</sup> force fields, respectively. The LINCS algorithm was used to constrain hydrogen bonds, and a time step of 2 fs was used. Long-range electrostatics were truncated with the force-switching method starting at  $r_{\text{on}} = 10 \text{ \AA}$  until  $r_{\text{off}} = 13 \text{ \AA}$ .<sup>15</sup>

During this initial equilibration phase, the distance between the pThr14  $\text{O}_\gamma$  on the Cdk2 leaving group and the acidic hydrogen from Glu474 on Cdc25B,  $d(\text{OH})$ , was noted to be too large for  $\text{H}^+$  transfer,  $d(\text{OH}) \approx 7 \text{ \AA}$ . The free energy associated with decreasing such a distance was determined. An umbrella potential was used to guide the  $d(\text{OH})$  coordinate toward lower values in a series of short simulations. The effect of such a potential was removed, and the short simulations were pieced together using the weighted histogram analysis method (WHAM).<sup>18</sup> Reference values  $\xi_i$  were equally spaced at  $0.10 \text{ \AA}$ , and a constant  $k_{\text{umb}} = 1500 \text{ kJ mol}^{-1} \text{ \AA}^{-2}$  was used. Molecular dynamics runs with at least 5 ps of equilibration and 20 ps of data collection were used for each reference window  $\xi_i$ . Further details are the same as those previously reported.<sup>8,19</sup>

Another 5 ns of molecular dynamics were run for equilibration of the solvated Michaelis complex. Harmonic potentials were used to tether the pThr14 phosphorus to the Cys473 sulfur and the pThr14  $\text{O}_\gamma$  oxygen to the Glu474 acidic hydrogen. Both harmonic potentials had minima set to  $4.0 \text{ \AA}$  with  $k_f = 50 \text{ kcal mol}^{-1} \text{ \AA}^{-2}$ . The final configuration has a root-mean-squared deviation (rmsd) of  $0.8 \text{ \AA}$  for all protein  $\text{C}_\alpha$  atoms in comparison with the initial structure provided by Rudolph.<sup>13</sup> This final equilibrated structure (Figure 1) represents a better model to study the possible phosphate and  $\text{H}^+$  transfers catalyzed by Cdc25B in complex with Cdk2-pTpY/CycA.

Free-energy profiles for the chemical reactions were obtained with a hybrid potential of quantum mechanics and molecular mechanics (QM/MM)<sup>20</sup> specifically parametrized for phosphatases.<sup>21</sup> This potential has already been tested extensively and shown to provide excellent agreement with experiment for another dual-specificity phosphatase, VHR, in wild-type and mutated forms, reacting either with aryl or alkyl small-molecule substrates.<sup>8,22</sup> In the hybrid potential simulations, the side chains of Cys473, Glu474, and pThr14 were represented in the QM region with the parametrized QM/MM potential.<sup>21</sup> The remainder of the protein complex and the solvent were represented with the OPLS-AA and TIP-3P force fields, respectively. A combination of an umbrella potential and the WHAM method was used

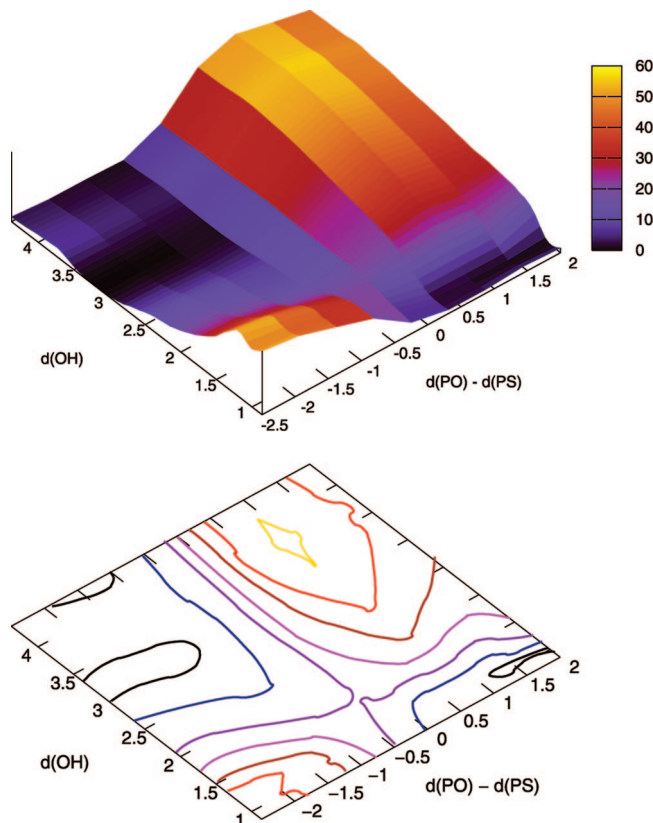


**Figure 2.** Two-dimensional free-energy profile (color coded in kcal/mol) for dephosphorylation of the Cdk2-pTpY/CycA complex by Cdc25B. The phosphate in pThr14 was modeled as a dianion.  $\text{H}^+$  transfer is represented by  $d(\text{OH})$ , the distance between the pThr14  $\text{O}_\gamma$  and the acidic hydrogen from Glu474. Phosphate transfer is described by  $d(\text{PO}) - d(\text{PS})$ , the difference between forming P-S and breaking P-O bonds to phosphorus. In the Michaelis complex,  $d(\text{PO}) - d(\text{PS}) < -1.5$ . In the product,  $d(\text{PO}) - d(\text{PS}) > +1.0$ . The upper panel is a 3D projection. The lower panel is a contour plot for the same data with discrete energy levels of 2, 7, 17, 27, 37, 47, and 57 kcal/mol, following the color code given in the upper panel.

to obtain the reaction free-energy profiles as described above. A velocity Verlet–Langevin scheme was used to integrate the equations of motion<sup>23</sup> during the simulation of reaction profiles. A time step of 1 fs and a friction coefficient of  $\gamma = 10 \text{ ps}^{-1}$  were used. Additional details are the same as those used in previous phosphatase simulations.<sup>8,21</sup>

Equilibration molecular dynamics were carried out with the GROMACS program (version 3.3.2).<sup>15</sup> Computations of free-energy profiles were done with the DYNAMO library.<sup>24</sup>

### 3. Results and Discussion

In the simulated Michaelis complex shown in Figure 1, the dianionic phosphate group of pThr14 is coordinated to the Cdc25B P-loop. The ionized phosphate equatorial oxygens are hydrogen bonded with the P-loop backbone and with the Arg479 side chain on Cdc25B. Such an arrangement is equivalent to the one observed for reaction of VHR phosphatase with small-molecule substrates.<sup>8</sup> The pThr14  $\text{O}_\gamma$  forms a hydrogen bond to the side chain of Arg36 on Cdk2. This last side chain together with the side chain in Phe475 on Cdc25B creates a pathway for proton transfer from Glu474. The average distance between Arg36 and Phe475 side chains observed during the last 1 ns of molecular dynamics in the equilibration phase is  $4.6 \text{ \AA}$ . It is enough space for the transferred  $\text{H}^+$  to travel from Glu474 to pThr14. Glu474  $\text{O}_\epsilon$  also forms a hydrogen bond to the Arg36

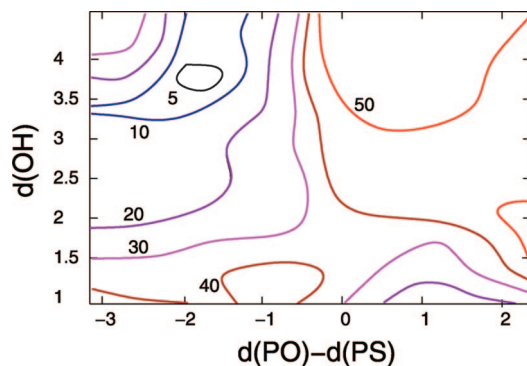


**Figure 3.** Two-dimensional free-energy contour plot (color coded in kcal/mol) for dephosphorylation of the Cdk2-pTpY/CycA complex catalyzed by Cdc25B with the phosphate group in pThr14 modeled as a monoanion. The  $d(\text{PO}) - d(\text{PS})$  is defined in Figure 2, and  $d(\text{OH})$  is the distance between the pThr14  $\text{O}_\gamma$  and the phosphate hydrogen.

side chain. Hence, the Arg36 side chain on Cdk2 is buried in the Cdc25B active site. Site-directed mutagenesis of this residue has not decreased phosphatase activity nor changed the  $k_{\text{cat}}/K_M$  versus pH profiles.<sup>13</sup> Thus, Arg36 on Cdk2 might not be important for the transition-state stabilization, but it seems relevant for complexation between Cdk2 and Cdc25B.

Figure 2 describes the energetics of two reaction coordinates representing  $\text{H}^+$  transfer and phosphate transfer. In the Michaelis complex,  $d(\text{OH}) < 3.0 \text{ \AA}$  and  $d(\text{PO}) - d(\text{PS}) < -1.5$ . In this region, the free-energy surface is flat, indicating that there is some conformational freedom for Glu474 and pThr14 side chains. Phosphate transfer from pThr14 would not occur without proton transfer to the leaving group. Figure 2 shows that barriers as high as 60 kcal/mol would have to be traversed if  $d(\text{OH}) > 2 \text{ \AA}$ . On the other hand, proton transfer to pThr14  $\text{O}_\gamma$  would not occur if the P–O bond in pThr14 was preserved, again because barriers are as high as 60 kcal/mol. Hence, both reactions are concerted. In the transition-state region,  $d(\text{OH}) \approx 1.5 \text{ \AA}$  and  $d(\text{PO}) - d(\text{PS}) \approx -0.3 \text{ \AA}$ . In the product region, the phosphate group is transferred to Cys473, Cdc25B is thiophosphorylated, and Cdk2 is dephosphorylated. The calculated free-energy barrier is 17 kcal/mol. This value is identical to the barrier determined experimentally.<sup>25</sup> In fact,  $\text{H}^+$  transfer is well-advanced, but not complete, in comparison to phosphate transfer in the transition state. This is in line with the interpretation of kinetic isotope effects measured for the dephosphorylation of an alkyl phosphate substrate by Cdc25A.<sup>26</sup>

The second proposal for general acid catalysis, namely, that pThr14 could bind as a phosphate monoanion and transfer the proton itself to the leaving group was tested on Figure 3. In the reactant state corresponding to the Michaelis complex, one of the equatorial phosphate oxygens in pThr14 is protonated, and the extra proton is coordinated by the Cys473 thiolate. The other interactions in the active site are similar to those described above for the dianion reaction. Phosphate and  $\text{H}^+$  transfer are concerted, with the transition state located in the region with  $d(\text{PO}) - d(\text{PS}) \approx -0.2 \text{ \AA}$  and  $d(\text{OH}) \approx 1.7 \text{ \AA}$ . The calculated free-energy barrier is 38 kcal/mol, indicating that this proposal is energetically unfeasible and that no reaction would be experimentally observed if the pThr14 phosphate group was protonated. Reaction barriers of similar magnitudes were also calculated for reaction of small-molecule substrates in monoanionic (monoprotonated) form with the VHR phosphatase.<sup>8</sup>

The simulation method used and the reaction barriers calculated here have a precision of  $\pm 5$  kcal/mol or better, as shown for another PTP.<sup>8,21</sup> Therefore and also because of the

**TABLE 1: Calculated Geometrical Parameters for Cdk2-pTpY/CycA Complexed with Cdc25B<sup>a</sup>**

	initial structure <sup>13</sup>	Michaelis complex
Glu474 Dihedrals		
$\text{HO}-\text{C}_\delta-\text{C}_\gamma-\text{C}_\beta$	173	50
$\text{C}_\delta-\text{C}_\gamma-\text{C}_\beta-\text{C}_\alpha$	-167	53
$\text{C}_\gamma-\text{C}_\beta-\text{C}_\alpha-\text{N}$	-178	43
	initial structure <sup>13</sup>	Michaelis complex
Distance Between		
$\text{HO}(\text{Glu474})^b$ $\text{O}_\gamma(\text{pThr14})^c$	7.2	4.1
$\text{O}_\gamma(\text{pThr14})^c$ $\text{H}_\omega(\text{Arg36})^c$	2.4	2.5
$\text{O}_\epsilon(\text{Glu474})^b$ $\text{H}_{(\omega')}(\text{Arg36})^c$	2.6	3.0
$\text{O}_\epsilon(\text{Glu474})^b$ $\text{H}_\omega(\text{Arg427})^b$	4.4	6.0
$\text{O}_\epsilon(\text{Glu474})^b$ $\text{H}^4(\text{Tyr528})^b$	1.6	3.4
$\text{O}_\epsilon(\text{Glu474})^b$ $\text{C}^4(\text{Phe475})^b$	4.2	3.2
$\text{C}_\delta(\text{Glu474})^b$ $\text{C}^4(\text{Phe475})^b$	4.5	4.2

<sup>a</sup> Distances given in  $\text{\AA}$ , and angles given in degrees. <sup>b</sup> On Cdc25B. <sup>c</sup> On Cdk2.

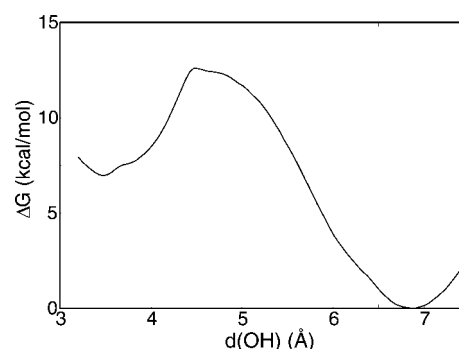


**Figure 4.** Free-energy profile (kcal/mol) for the conformational transition that decreases the distance between the Cdk2 pThr14  $\text{O}_\gamma$  and the acidic hydrogen from Glu474 on Cdc25B,  $d(\text{OH})$ .

agreement between the calculated barrier for reaction of pThr14 in dianionic form with experimental measurements (see above), it can be concluded that Glu474 on Cdc25B may well function as the catalytic general acid in dephosphorylation of its natural substrate, pThr14 on the Cdk2-pTpY/CycA complex.

As mentioned in the Materials and Methods section, the distance between pThr14  $\text{O}_\gamma$  and the acidic hydrogen from Glu474 observed in the initial structure<sup>13</sup> was too large for  $\text{H}^+$  transfer (see Table 1). It is shown in Figure 4 that the conformational transition associated with this distance reduction is accessible. Simulations show that this transition corresponds to torsions of the Glu474 side chain dihedrals, with the reminder of the protein complex showing no appreciable structural deviations. Relevant geometrical parameters are given in Table 1. The Glu474 side chain switches from an extended trans conformation at  $d(\text{OH}) \approx 7 \text{ \AA}$  to a gauche conformation at  $d(\text{OH}) \approx 4 \text{ \AA}$ . The calculated free-energy profile shown in Figure 4 has a free-energy barrier of 12 kcal/mol for reaction from right to left. Thus, the Glu474 side chain is flexible, and the transition that approximates the acidic hydrogen to the leaving group is thermally accessible at room temperature. It has been proposed that a related conformational transition could be rate-limiting in the Cdc25-catalyzed dephosphorylation of small-molecule substrates containing leaving groups with high  $\text{pK}_a$ 's.<sup>11</sup> However, the simulations presented here indicate that the chemical step is slower than the Glu474 conformational transition. Nevertheless, the free-energy difference between the right and left minima, 7 kcal/mol, should be added to the



reaction barrier calculated for the dianion reaction (Figure 2). Measured reaction rates are related to the lowest accessible free-energy minima and the top of the barrier.

Table 1 also shows interactions of Glu474 that may be explored in the rational design of inhibitors to Cdc25s. For instance, a possible inhibitor could push the Glu474 side chain away from the Cdc25B active site in the direction of Arg427. Then, Glu474 O<sub>ε</sub> could hydrogen bond to the side chains of either Arg427 and Tyr528. In fact, a hydrogen bond is already formed between Glu474 and Tyr528 side chains in the initial structure. A putative inhibitor could prevent disruption of this last hydrogen bond, preserving a favorable energetic contact and, hence, block the conformational transition that decreases *d*(OH) and allows general acid catalysis. Such an inhibitor could also benefit from  $\pi$ -stacking interactions with Phe475.

The present study gives compelling evidence that Glu474 on Cdc25B, or the equivalent amino acid in other Cdc25 isoforms, performs as the general acid for dephosphorylation of its natural substrate. The different identity and location of this general acid on Cdc25 from other PTPs can be explored in the design of specific inhibitors. Actually, we believe this is a new and important strategy to design specific inhibitors for Cdc25 phosphatases. This inhibitory mechanism would involve obstruction of Glu474 side chain flexibility, avoiding the general acid to get close enough to the substrate leaving group for H<sup>+</sup> transfer. In fact, a related possibility has already been explored with success for phosphatase Ptp1B. A conformational transition of the WPD loop in Ptp1B that correctly places the catalytic general acid was blocked by small molecules.<sup>27</sup> We are now exploring similar inhibitory strategies in our laboratory.

**Acknowledgment.** The author would like to acknowledge funding from FAPESP (Fundação de Amparo a Pesquisa do Estado de São Paulo, Projects 07/52772-6 and 07/59345-6).

## References and Notes

- (1) Lyon, M. A.; Ducruet, A. P.; Wipf, P.; Lazo, J. S. *Nat. Rev. Drug Discovery* **2002**, *1*, 961–976.
- (2) Ducruet, A. P.; Vogt, A.; Wipf, P.; Lazo, J. S. *Annu. Rev. Pharmacol. Toxicol.* **2005**, *45*, 725.

- (3) Jiang, Z.-X.; Zhang, Z.-Y. *Cancer Metastasis Rev.* **2008**, *27*, 263–272.
- (4) Contour-Galcerà, M.-O.; Sidhu, A.; Prvost, G.; Bigg, D.; Ducommun, B. *Pharmacol. Ther.* **2007**, *115*, 1–12.
- (5) Robertson, J. G. *Biochemistry* **2005**, *33*, 5561–5571.
- (6) Rudolph, J. *Biochemistry* **2007**, *46*, 3595–3604.
- (7) Jackson, M. D.; Denu, J. M. *Chem. Rev.* **2001**, *101*, 2313–2340.
- (8) Arantes, G. M. *Biochem. J.* **2006**, *399*, 343–350.
- (9) Fauman, E. B.; Cogswell, J. P.; Lovejoy, B.; Rocque, W. J.; Holmes, W.; Montana, V. G.; Piwnicka-Worms, H.; Rink, M. J.; Saper, M. A. *Cell* **1998**, *93*, 617–625.
- (10) Reynolds, R. A.; Yem, A. W.; Wolfe, C. L.; Deibel, M. R.; Chidester, C. G.; Watenpaugh, K. D. *J. Mol. Biol.* **1999**, *293*, 559–568.
- (11) McCain, D. F.; Catrina, I. E.; Hengge, A. C.; Zhang, Z.-Y. *J. Biol. Chem.* **2002**, *277*, 11190–11200.
- (12) Rudolph, J. *Biochemistry* **2002**, *41*, 14613–14623.
- (13) Sohn, J.; Parks, J. M.; Buhman, G.; Brown, P.; Kristjansdottir, K.; Safi, A.; Edelsbrunner, H.; Yang, W.; Rudolph, J. *Biochemistry* **2005**, *44*, 16563–16573.
- (14) Field, M. J. *A Practical Introduction to the Simulation of Molecular Systems*, 1st ed.; Cambridge University Press: Cambridge, U.K., 1999.
- (15) Lindahl, E.; Hess, B.; van der Spoel, D. *J. Mol. Model.* **2001**, *7*, 306–317.
- (16) Jorgensen, W. L.; Maxwell, D. S.; Tirado-Rives, J. *J. Am. Chem. Soc.* **1996**, *118*, 11225–11236.
- (17) Jorgensen, W. L.; Chandrasekhar, J.; Madura, J. D.; Impey, R. W.; Klein, M. L. *J. Chem. Phys.* **1983**, *79*, 926–935.
- (18) Roux, B. *Comput. Phys. Commun.* **1995**, *91*, 275–282.
- (19) Thomas, A.; Jourand, D.; Bret, C.; Amara, P.; Field, M. J. *J. Am. Chem. Soc.* **1999**, *121*, 9693–9702.
- (20) Field, M. J.; Bash, P. A.; Karplus, M. *J. Comput. Chem.* **1990**, *11*, 700–733.
- (21) Arantes, G. M.; Loos, M. *Phys. Chem. Chem. Phys.* **2006**, *8*, 347–353.
- (22) Arantes, G. M. On the Protein Tyrosine Phosphatases. Phosphate Esters Intrinsic Reactivity and Computer Simulation of the Mechanisms of Enzymatic Reaction. Thesis, Institute of Chemistry, University of São Paulo, 2004.
- (23) Allen, M.; Tildesley, D. *Computer Simulation of Liquids*, 1st ed.; Oxford University Press: New York, 1987.
- (24) Field, M. J.; Albe, M.; Bret, C.; Martin, F. P.-D.; Thomas, A. *J. Comput. Chem.* **2000**, *21*, 1088–1100.
- (25) Sohn, J.; Rudolph, J. *Biophys. Chem.* **2007**, *125*, 549–555.
- (26) McCain, D. F.; Grzyska, P. K.; Wu, L.; Hengge, A. C.; Zhang, Z.-Y. *Biochemistry* **2004**, *43*, 8256–8264.
- (27) Wiesmann, C.; Barr, K. J.; Kung, J.; Zhu, J.; Erlanson, D. A.; Shen, W.; Fahr, B. J.; Zhong, M.; Taylor, L.; Randal, M.; McDowell, R. S.; Hansen, S. K. *Nat. Struct. Mol. Biol.* **2004**, *11*, 730–737.

JP8070019